OPEN ACCESS

polymers

Article

Evaluation of the Biological Effects of Externally Tunable, Hydrogel Encapsulated Quantum Dot Nanospheres in *Escherichia coli*

Somesree GhoshMitra [1], Tong Cai [2], David Diercks [3], Zhibing Hu [2], James Roberts [2], Jai Dahiya [4], Nathaniel Mills [1], DiAnna Hynds [1] and Santaneel Ghosh [4],*

[1] Department of Biology, Texas Woman's University, Denton, TX 76204, USA;
E-Mails: sghoshmitra@mail.twu.edu (S.G.); NMills@mail.twu.edu (N.M.);
Dhynds@mail.twu.edu (D.H.)

[2] Department of Physics, University of North Texas, Denton, TX 76203, USA;
E-Mails: tong.cai@gmail.com (T.C.); zbhu@unt.edu (Z.H.); roberts@unt.edu (J.R.)

[3] Metallurgical and Materials Engineering Department, Colorado School of Mines, Golden, CO
80401, USA; E-Mail: ddiercks@mines.edu (D.D.)

[4] Department of Physics and Engineering Physics, Southeast Missouri State University,
Cape Girardeau, MO 63701, USA; E-Mail: jndahiya@semo.edu (J.D.)

* Author to whom correspondence should be addressed; E-Mail: sghosh@semo.edu;
Tel.: +1-573-651-2393; Fax: +1-573-651-2392.

Abstract: Quantum Dots (QDs) have become an interesting subject of study for labeling and drug delivery in biomedical research due to their unique responses to external stimuli. In this paper, the biological effects of a novel hydrogel based QD nano-structure on *E. coli* bacteria are presented. The experimental evidence reveals that cadmium telluride (CdTe) QDs that are encapsulated inside biocompatible polymeric shells have reduced or negligible toxicity to this model cell system, even when exposed at higher dosages. Furthermore, a preliminary gene expression study indicates that QD-hydrogel nanospheres do not inhibit the Green Fluorescent Protein (GFP) gene expression. As the biocompatible and externally tunable polymer shells possess the capability to control the QD packing density at nanometer scales, the resulting luminescence efficiency of the nanostructures, besides reducing the cytotoxic potential, may be suitable for various biomedical applications.

---

1. Introduction

Innovative approaches possessing novel therapeutic potential need to be implemented in order to overcome the existing challenges for early diagnosis and treatment of significant health burdens (e.g., cancer). An area of nanotechnology that holds huge promise for probing the details of cellular and molecular processes in cells is application of surface engineered QDs. Recently, QDs are being used extensively for labeling [1-8] in biomedical research due to their unique photoluminescence properties: (1) size-tunable emission color, (2) a narrow and symmetric emission profile and (3) a broad excitation range. At the same time, based on excellent biological compatibility, adaptability to pH and temperature changes, as well as responsiveness to magnetic or electric fields, hydrogel nanospheres have become suitable carriers for drugs, fluorescent labels, magnetic particles for hyperthermia applications, and particles that have strong absorption profiles for optical excitation [7,9-12]. Therefore, integration of fluorescent, water-soluble QDs into hydrogel nanospheres provides a new generation of fluorescence markers for biological assays. Incorporation of same size and/or differently sized nanocrystals (NCs) into one bead may provide new pathways for fast and early detection systems since the emission spectra of QDs can be tuned to match practically any energy acceptor molecule by tailoring the size, shape, and composition of the QDs. Moreover, for a thermo-responsive polymer based QD system, the polymer shell acts as the reservoir of the drug molecules plus a tunable biocompatible matrix around the QDs, and thus controls the distance between the adjacent dots inside the nanospheres. Therefore, the possibility of external modulation to bring the dots close enough to cause Förster resonance energy transfer (FRET) makes it an attractive alternative for biological detection that overcomes traditional difficulties in actuating conventional micro- or nanostructures by chemical, mechanical or magnetic excitations [11,13].

Cadmium chalcogenide QDs provide the most attractive fluorescent labels in comparison with routine dyes or metal complexes [14,15]. However, the excellent optical properties of CdTe QDs have not translated into a biomedical breakthrough in tumor imaging devices or "*theragnostics*" applications. A major hurdle is that uncoated QDs made of CdTe are toxic to cells because of release of Cd^{2+} ions and reactive oxygen species (ROS) generation into the cellular environment [14,16-22]. This problem can be partially solved by encapsulating QDs with hydrophilic polymers, like poly(N-isopropylacrylamide) (PNIPAM) or poly(ethylene glycol) (PEG) [15,23]. The toxicity of uncoated QDs is known; however, only a very limited number of studies [15,23] have been specially designed to assess thoroughly the toxicity of nanosphere encapsulated QDs against QD density and dosing level. As hydrogel encapsulated quantum dots might be utilized in constructing future, novel systems for therapeutic applications, it is important to assess the toxicity profile of this platform.

In this work, we present studies of the biological effects of a novel CdTe-PNIPAM based nanomaterial system on *E. coli* bacteria. Hydrogels based on PNIPAM are well known thermoresponsive polymers that undergo a volume phase transition across the lower critical solution temperature (LCST), close to the normal physiological temperature, ~33 °C [9]. Therefore, the inherent temperature-sensitive volumetric transition properties of PNIPAM offer the potential to

control QD proximity within the nanospheres for *in vitro* or *in vivo* applications. As the CdTe QD toxicity has the ability to effectively kill *E. coli* bacteria by impairing the cell's anti-oxidative system, this serves as a cellular model to assess the toxicity profile of the hydrogel encapsulated QD nanospheres [24,25]. The existing reports have assessed single QD core-shell polymeric structure's toxicity where traditional polymer encapsulation is not externally tunable, and cannot control the intermediate distance between the adjacent dots and is not suitable for drug delivery applications in which triggered release is necessary. Thus, the scarcity of information on the biocompatibility and organelle specific labeling by tunable polymer-QD bio-conjugates prompted this study of CdTe-PNIPAM nanoreservoirs. Moreover, this system has the potential to be formulated as a novel antimicrobial material with excellent optical properties. Thus, evaluation of biological effects on *E. coli* is extremely necessary.

2. Experimental Section

Nanogel encapsulated QDs were synthesized by first preparing PNIPAM nanospheres through precipitation polymerization of N-isopropylacrylamide monomer and methylene-bis-acrylamide (BIS) as a crosslinker and CdTe QDs capped with a stabilizer. The CdTe QDs were bonded into PNIPAM nanogels through the replacement of CdTe's stabilizer inside PNIPAM nanospheres. Scanning Electron Microscopy (SEM) was used to observe size and morphology of the hydrogel particles. Growth curves were generated for *E. coli* growing in 20 mL of Luria-Bertani (LB) media containing hydrogel encapsulated QD nanospheres (~400 nm diameter) at relatively higher (1.0–0.3 mg/mL) and lower (0.25–0.05 mg/mL) gel concentrations. A preliminary gene expression study was conducted by transforming *E. coli* cells with plasmid pGLO, which express green fluorescent protein (GFP).

2.1. Synthesis of CdTe-PNIPAM Nanospheres

PNIPAM encapsulated QD nano-spheres were synthesized in three steps [26]. This three-step process consists of (1) PNIPAM particle synthesis; (2) CdTe nanocrystal preparation; (3) encapsulation of nanocrystals in PNIPAM nano spheres. Specifically, PNIPAM particles were synthesized by mixing NIPAM monomer, N(3-aminopropyl) methylacrylamide chloride monomer, methylene-bis-acrylamide and N,N-cysteine-bis-acrylamide in deionized, distilled water. The solution was sparged with nitrogen and heated to 70 °C for 40 min. Potassium persulfate was then added to the solution to initiate the reaction. The reaction was carried out at 70 °C for 4 h. CdTe nanocrystals were synthesized from sodium hydrogen telluride (NaHTe) and $Cd(ClO_4)_2 \cdot 6H_2O$ with proper pH adjustment. PNIPAM encapsulated QDs were synthesized by breaking the S-S bonds and forming reactive thiol groups and cross-linking those with free thiols on the QDs. PNIPAM particles were mixed with 1,4-dithiothreitol to break S-S bonds and to form reactive thiol groups. The mixed solutions (PNIPAM particles and the QDs, 24 h) were centrifuged at 3,000–10,000 rpm for 1 h at 25 °C. By decanting the supernatant, followed by repeating the cycle of re-dispersion with water and centrifugation (six to eight times), the unloaded and surface attached QDs were removed and PNIPAM spheres loaded with CdTe QDs were obtained, denoted as CdTe-PNIPAM. It is observed that after four washings, almost all surface attached QDs get detached. A schematic is provided in Figure 1.

Figure 1. CdTe-PNIPAM nanosphere synthesis and temperature responsive behavior.
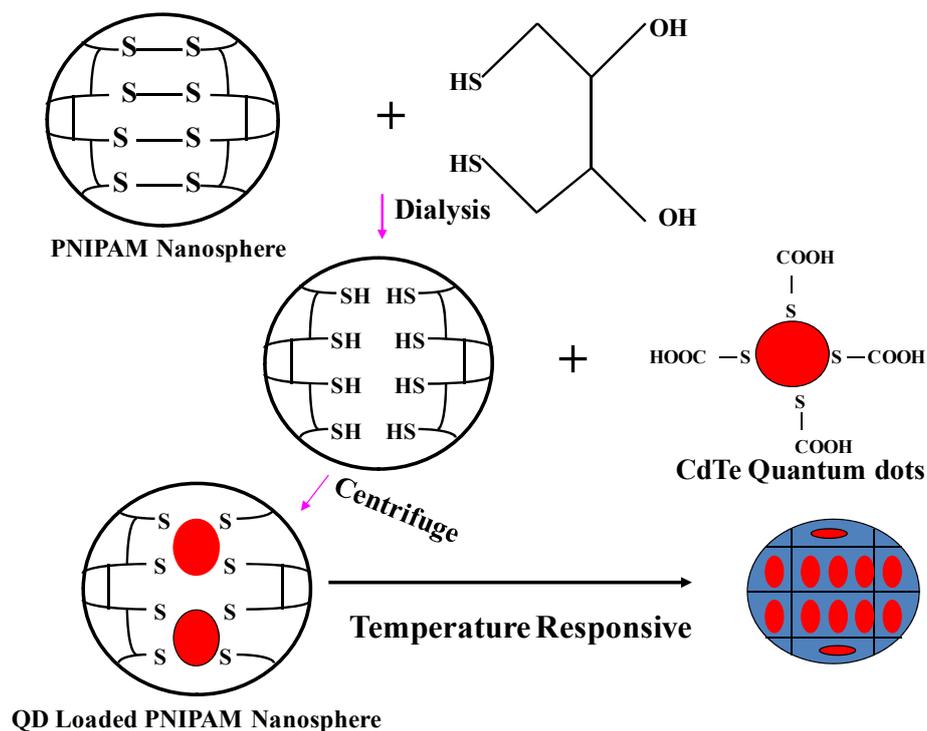
2.2. Scanning and Transmission Electron Microscopy (SEM and TEM)

An FEI Nova Nanolab 200 Scanning Electron Microscope (SEM) was used to observe the morphology of the hydrogel encapsulated quantum dot nanospheres. In order to prevent collapsing of the polymer network, cryo-immobilization was achieved through plunge-cooling the sample in liquid nitrogen. Accelerating voltage for SEM imaging was kept between 20–30 kV, which enables secondary electron signal generation from the sample. SEM imaging was performed at a magnification of ~120,000×. To observe the encapsulated QD nanocrystals, high resolution transmission electron microscopy (HRTEM) was carried out using an FEI Tecnai F20 HRTEM.

2.3. Bacterial Cell Culture

E. coli (K 12) was grown aerobically at 37 °C in an incubator/shaker at 100 rpm overnight to stationary phase. Luria-Bertani (LB) medium (10 gm/L of Tryptone, 5 gm/L yeast extract and 10 gm/L sodium chloride) was used for the bacterial culture. A small but equal amount of saturated culture (1:100 by volume) was seeded into each freshly prepared PNIPAM-QD-LB Broth solution. For spectrophotometric reference, unseeded PNIPAM-LB Broth solutions were used. The positive control was the same growth media without PNIPAM-QD nanospheres. These cultures were incubated at 37 °C, shaking at 100 rpm and the optical density (OD) was measured using A_{600nm} at selected times to determine growth rates. 600 nm is selected, because to measure bacterial growth by light scattering it is best to pick a wavelength where absorption is at a minimum and for most bacterial cultures wavelengths around 600 nm are a good choice [24]. This procedure was followed for all concentrations of QD/PNIPAM gels evaluated.

2.4. Transformation of E. coli *with pGLO*

E. coli K 12 cells were made competent using treatment with a calcium chloride solution. The transformation process introduced a commercial 5.4 kb plasmid encoding green fluorescent protein (GFP) regulated by an arabinose promoter and conferring ampicillin resistance (pGLO, BioRad, Inc., Hercules, CA, USA). Transformed cells were re-suspended in the nutrient broth and spread on plates containing LB agar, ampicillin, and arabinose, and then incubated at 37 °C overnight. Another control plate was streaked using LB and ampicillin, without arabinose. Both plates contained 100 µL PNIPAM-QD nanosphere solutions. LB-Amp-Ara plates without nanospheres were used as a positive control.

3. Results and Discussion

3.1. Physicochemical characterization of CdTe-PNIPAM Nanospheres

The QD-PNIPAM nanospheres exhibited good colloidal stability in aqueous solution with excellent luminescent efficiency and no obvious precipitation after several days (Figure 2(A)). Under proper storage conditions (2–6 °C, in a dark vial) the nanospheres can be stored for up to two years. In order to extract the nanosphere morphology and size distribution, scanning electron microscopy (SEM) was performed. The sample preparation involved plunge cooling inside liquid nitrogen, thus preventing them from collapsing after freeze-drying. Spherical to oval shaped particles were observed (Figure 2(B)); analyzing several images and constructing the nanosphere size distribution histogram (not shown here), the mean diameter was found to be 382 ± 45 nm, which was re-confirmed by the Dynamic Light Scattering (DLS) measurement.

Figure 2. (A) Luminescent CdTe-PNIPAM nanospheres. **(B)** SEM micrograph of the CdTe-PNIPAM nanospheres demonstrating polymer encapsulation and sphere morphology (scale bar = 300 *nm*). **(C)** HRTEM micrograph of the encapsulated CdTe QDs inside the PNIPAM shell (scale bar = 10 nm).
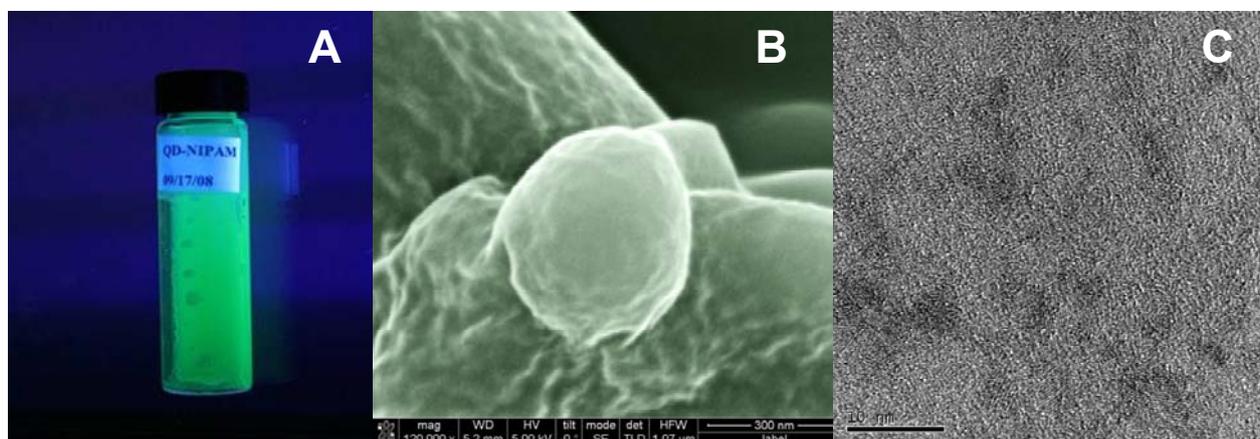
It should be noted that, during sample preparation for SEM imaging, some spheres become slightly oval shaped because of surface roughness of the carbon tape (on the mounting stub, seen in the background). It is important for the designed system that the polymer encapsulates the nano-sized QDs, which not only facilitate the solubility and bioavailability, but also provides a linker for bioconjugation of peptides, antibodies, oligonucleotides, or small molecule drugs. The SEM micrographs did not reveal any QD nanocrystals on the surface of the hydrogel nanoparticles. The absence of QDs on the surface provided indirect proof of the polymer encapsulation around the semiconductor nanocrystals and not surface attachment, which is extremely important for biomedical applications. The lower electron beam energy (5–30 kV) of SEM imaging was insufficient to penetrate the outer polymer shell, so we directly assessed particle encapsulation by HRTEM. At an accelerating voltage of 200 kV, electrons were able to pierce through the outer polymer shell. Using Performing High Resolution Transmission Electron Microscopy (HRTEM) analysis (not shown here), the loading of CdTe QDs was found as $\sim 0.4 \times 10^4$ inside a typical 400 nm diameter PNIPAM sphere for the medium density packing. For high and low density packed spheres, these numbers stand at $\sim 0.7 \times 10^4$ and 0.2×10^4 per sphere, respectively. HRTEM micrographs (Figure 2(C)) further reveal that the QDs did not form large scale agglomerations and were quite uniformly distributed throughout the spheres. The average QD diameter was found to be 2.5 ± 0.2 nm, excitation wavelength was 400 nm, and the emission maximum was 530 nm. Simultaneous imaging of the polymer shell and the encapsulated QDs were not possible here. The problem in imaging core-shell nanostructures has been reported by other research groups as well [27,28]. It should be noted that, in our previous work, the QDs encapsulated in the PNIPAM nanospheres showed a 200% enhancement in the PL efficiency as the nanogels shrank at a temperature above the LCST of PNIPAM [26]. This PL enhancement is presumably due to the change of the configuration of the nanogels that confined the movement of QDs. The temperature induced refractive index change also led to a novel gain mechanism in these systems. It is suspected that the dots come closer once the temperature goes above the LCST, moving into the range of FRET.

To address concerns regarding nanosphere stability in the growth media, DLS measurements were taken of the nanospheres in distilled water and in LB growth media. With this procedure, the difference between the behavior of the nanospheres in solutions with and without salt was compared. We did not see any difference in diameter. Furthermore, as the nanoparticles have a tendency to agglomerate in LB media, we have performed a time dependent size measurement experiment. PNIPAM-coated QDs remained stable in LB media, thus retaining their size without forming large agglomerates. DLS measurements were taken over the time frame correlating with the growth measurements to determine how the particles behaved during that process. Figure 3 reveals DLS measurements of QD-PNIPAM nanospheres in suspension for a duration of five hours in LB media. During this run, the nanospheres remained stable and showed little change in hydrodynamic radius. Stability of PEG coated gold particles in LB media has previously been observed as well [24].

Figure 3. DLS measurements of QD-PNIPAM nanospheres during a time course of six hours in LB media. During this run, the nanospheres remain stable, and showed little changes in hydrodynamic diameter. N = 3, ±SD.
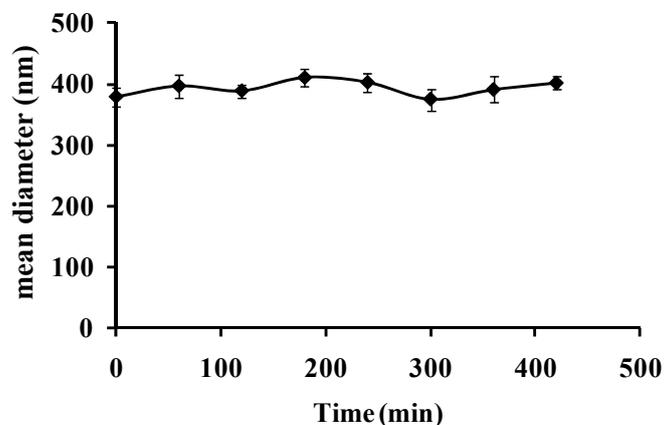
3.2. Microbial Growth Experiments and GFP Expression

Growth curves (Figure 4(A–C)) were generated for *E. coli* growing in 20 mL of LB media containing QD-PNIPAM nanospheres (400 nm diameter) with high, medium, and low packing densities. For each loading scenario, toxic (red), borderline (blue), and safe (green) limits have been evaluated.

Figure 4. (A) Growth curve for *E. coli* for high packing density QD-PNIPAM nanospheres. **(B)** Growth curve for *E. coli* for medium packing density QD-PNIPAM nanospheres. **(C)** Growth curve for *E. coli* for low packing density QD-PNIPAM nanospheres. N = 3, ±SD.
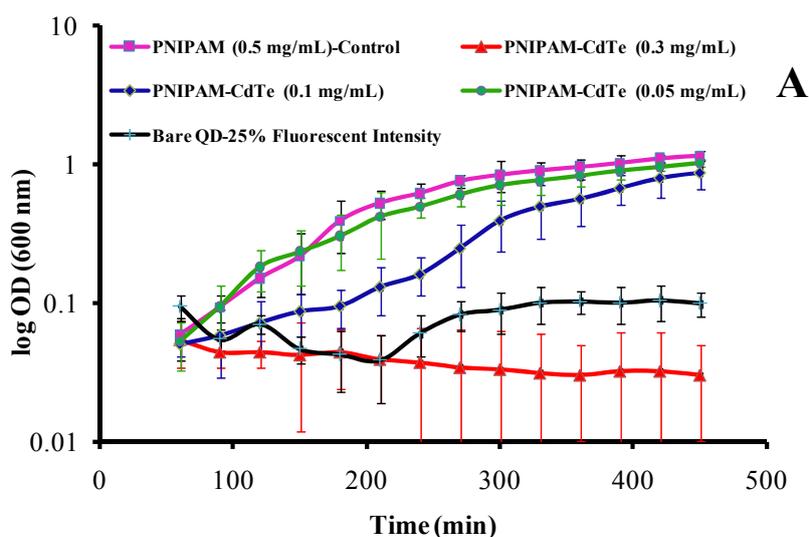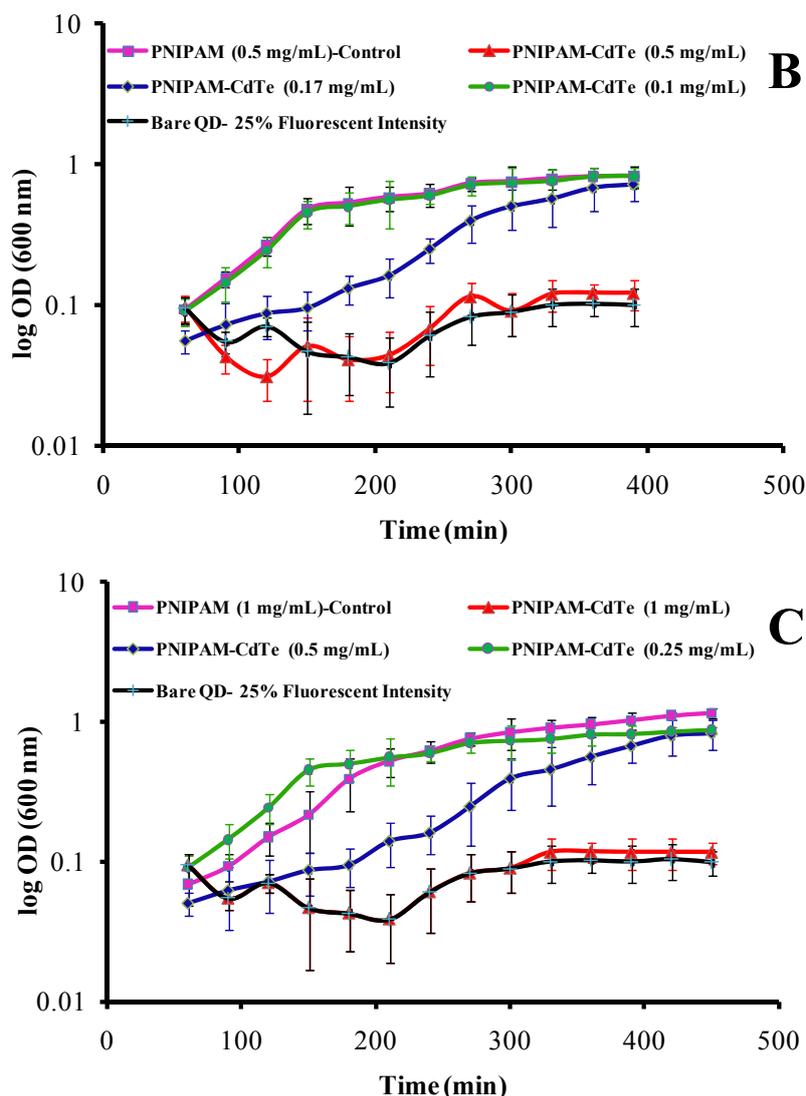
Figure 4. *Cont.*

The overall results indicate that even densely packed QD-PNIPAM spheres exhibit a safe limit (around 0.1 mg/mL) for *E. coli* growth. Uncoated CdTe solution having 25% fluorescent intensity to that of the low packing density nanospheres (borderline level, *i.e.*, 0.5 mg/mL) is used as negative control and growth rate is compared (black). It is observed that the encapsulated CdTe-PNIPAM nanospheres reduce cytotoxicity effects significantly. This is a significant improvement over the existing findings with QD cytotoxicity studies [20]. Although Helbig and coworkers have observed *E. coli* growth at a relatively higher Cd concentration [29], it must be noted that CdTe QDs (encapsulated or bare) are a completely different system. The reason for high dosages of Cd (75 µM) permitting *E. coli* growth may be related to lower intracellular uptake of the Cd^{2+} ions in the absence of surface modification and subsequently, less ROS generation. Moreover, QD size and surface charge has played a huge role in toxicity and uptake, as observed by Lovric and coworkers [30]. In our study, the growth of *E. coli* exposed to significantly higher concentration was inhibited but at moderate or lower concentration, the growth was normal. This is particularly important for high density packing, as the dots are close to each other and volumetric shrinkage of the PNIPAM shell brings them even closer at temperatures above the LCST, thus the condition becomes ideal for FRET. For medium and low packed

QD-PNIPAM spheres, higher concentration levels (0.17 mg/mL for medium packed and 0.5 mg/mL for low packed) proved to have negligible cytotoxic effects. Bacterial growth depends on available nutrition and environment. At higher QD concentrations the mechanism for growth inhibition may be that quantum dots have some effects on replication machinery, slowing DNA synthesis and leading to increased time before binary fission.

A preliminary gene expression study was conducted by transforming *E. coli* cells with plasmid pGLO, which expresses GFP. Green fluorescent colonies were observed after overnight incubation of spread LB-amp-ara plates with a high density QD-PNIPAM nanospheres (0.1 mg/mL, borderline level) (Figure 5(A)). Encapsulated CdTe QDs did not suppress arabinose promoter regulated pGLO gene product GFP expression. A similar number of fluorescent colonies were present in the positive control (without nanospheres, not shown here); however, cell growth was prohibited drastically with bare QDs, even from dosages having as low as one-fourth of the fluorescent intensity as that of the previously administered PNIPAM encapsulated QDs. As a result, no colony formation took place and no signal was detected (not shown). Similar results (about 50% inhibition ratios after 135 min exposure) were observed during toxicological assessment of TiO_2 nanoparticles with recombinant *E. coli* [25]. This indicates that the PNIPAM-QD nanospheres are not cytotoxic to the procaryotic cells at certain concentrations and do not inhibit the GFP gene expression. Furthermore, healthy cells were observed (Figure 5(B)) after overnight incubation with high density QD-PNIPAM nano-spheres at this dose level; again cell growth was not observed with bare QD exposure (previously mentioned dose level).

Figure 5. (A) *E. coli* with pGLO expressing green fluorescent protein in the presence of QD-PNIPAM nanospheres (high packing density, 0.1 mg/mL PNIPAM concentration). **(B)** SEM image of *E. coli* growth in the presence of QD-PNIPAM nanospheres (high packing density, 0.1 mg/mL PNIPAM concentration, overnight incubation).
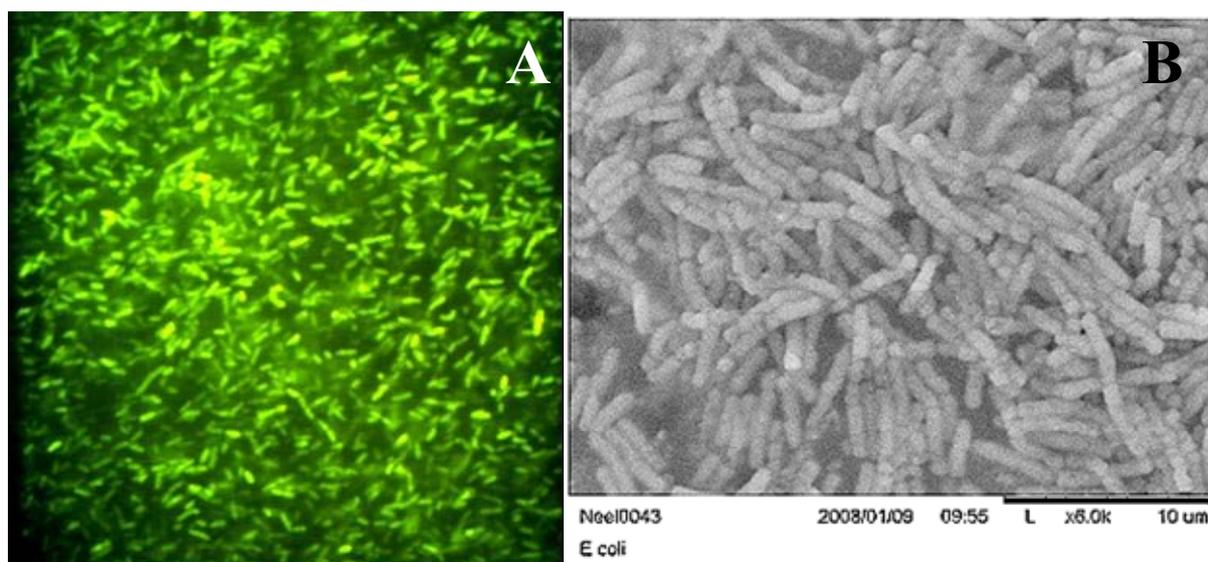
4. Conclusions

In the present work, *E. coli* growth was monitored as a representation of how cells might respond in the presence of hydrogel encapsulated QDs in their growth environment. The CdTe QDs were successfully encapsulated in the PNIPAM gel network. From the growth curves, there was no evidence, at the certain concentrations tested, that the hydrogel encapsulated QDs prevented the microbial cells from growing. Of course, it is possible that there may be more subtle changes in cell function and behavior detectable only at the gene or protein level. However, the preliminary gene expression study indicated that QD-hydrogel nanospheres do not inhibit the GFP gene expression. Thus, the experimental evidence shows that CdTe QDs, if appropriately coated by a tunable biopolymer shell, like PNIPAM, induce much less toxicity (negligible below the critical concentration) to the model cell system studied here, even when exposed to higher dosages. These experimentally obtained results indicate that PNIPAM coated CdTe QDs are a promising alternate to uncoated QDs. Coupled with the externally tunable dot distribution capabilities derived from the PNIPAM networks [22,24], this novel nanoplatform may be useful for combinatorial therapeutics. We are currently assessing optically modulated responses of several neuronal models to the bio-conjugated nanospheres.

References

1. Alivisatos, P. The use of nanocrystals in biological detection. *Nat. Biotechnol.* **2004**, *22*, 47-52.
2. Niemeyer, C.M. Nanoparticles, proteins, and nucleic acids: Biotechnology meets materials science. *Angew. Chem. Int. Ed.* **2001**, *40*, 4128-4158.
3. Bagalkot, V.; Zhang, L.; Levy-Nissenbaum, E.; Jon, S.; Kantoff, P.W.; Langer, R.; Farokhzad, O.C. Quantum dot-aptamer conjugates for synchronous cancer imaging, therapy, and sensing of drug delivery based on bi-fluorescence resonance energy transfer. *Nano Let.* **2007**, *7*, 3065-3070.
4. Bakalova, R.; Ohba, H.; Zhelev, Z.; Ishikawa, M.; Baba, Y. Quantum dots as photosensitizers? *Nat. a-z Index* **2004**, *22*, 1360-1361.
5. Ballou, B.; Ernst, L.A.; Andreko, S.; Harper, T.; Fitzpatrick, J.A.J.; Waggoner, A.S.; Bruchez, M.P. Sentinel lymph node imaging using quantum dots in mouse tumor models. *Bioconjugate Chem.* **2007**, *18*, 389-396.
6. Bruchez, M., Jr.; Moronne, M.; Gin, P.; Weiss, S.; Alivisatos, A.P. Semiconductor nanocrystals as fluorescent biological labels. *Science* **1998**, *281*, 2013-2016.

7. GhoshMitra, S.; Diercks, D.R.; Mills, N.C.; Hynds, D.A.L.; Ghosh, S. Excellent biocompatibility of semiconductor quantum dots encased in multifunctional poly(N-isopropylacrylamide) nanoreservoirs and nuclear specific labeling of growing neurons. *Appl. Phys. Lett.* **2011**, *98*, 103702.

8. Smith, A.M.; Ruan, G.; Rhyner, M.N.; Nie, S. Engineering luminescent quantum dots for *in vivo* molecular and cellular imaging. *Ann. Biomed. Eng.* **2006**, *34*, 3-14.

9. Hu, Z.; Chen, Y.; Wang, C.; Zheng, Y.; Li, Y. Polymer gels with engineered environmentally responsive surface patterns. *Nature* **1998**, *393*, 149-152.

10. Ghosh, S.; GhoshMitra, S.; Cai, T.; Diercks, D.R.; Mills, N.C.; Hynds, D.A.L. Alternating magnetic field controlled, multifunctional nano-reservoirs: Intracellular uptake and improved biocompatibility. *Nanoscale Res. Lett.* **2010**, *5*, 195-204.

11. Garner, B.W.; Cai, T.; Ghosh, S.; Hu, Z.; Neogi, A. Refractive index change due to volume-phase transition in polyacrylamide gel nanospheres for optoelectronics and bio-photonics. *Appl. Phys. Express* **2009**, *2*, 057001.

12. Agrawal, M.; Rubio-Retama, J.; Zafeiropoulos, N.; Gaponik, N.; Gupta, S.; Cimrova, V.; Lesnyak, V.; Lopez-Cabarcos, E.; Tzavalas, S.; Rojas-Reyna, R. Switchable photoluminescence of CdTe nanocrystals by temperature-responsive microgels. *Langmuir* **2008**, *24*, 9820-9824.

13. Ghosh, S.; Yang, C.; Cai, T.; Hu, Z.; Neogi, A. Oscillating magnetic field-actuated microvalves for micro-and nanofluidics. *J. Phys. D* **2009**, *42*, 135501.

14. Derfus, A.M.; Chan, W.C.W.; Bhatia, S.N. Probing the cytotoxicity of semiconductor quantum dots. *Nano Lett.* **2004**, *4*, 11-18.

15. Zhang, T.; Stilwell, J.L.; Gerion, D.; Ding, L.; Elboudwarej, O.; Cooke, P.A.; Gray, J.W.; Alivisatos, A.P.; Chen, F.F. Cellular effect of high doses of silica-coated quantum dot profiled with high throughput gene expression analysis and high content cellomics measurements. *Nano Lett.* **2006**, *6*, 800-808.

16. Cho, S.J.; Maysinger, D.; Jain, M.; Röder, B.; Hackbarth, S.; Winnik, F.M. Long-term exposure to CdTe quantum dots causes functional impairments in live cells. *Langmuir* **2007**, *23*, 1974-1980

17. Hardman, R. A toxicologic review of quantum dots: Toxicity depends on physicochemical and environmental factors. *Environ. Health Perspect.* **2006**, *114*, 165-172.

18. Hoshino, A.; Manabe, N.; Fujioka, K.; Suzuki, K.; Yasuhara, M.; Yamamoto, K. Use of fluorescent quantum dot bioconjugates for cellular imaging of immune cells, cell organelle labeling, and nanomedicine: Surface modification regulates biological function, including cytotoxicity. *J. Artif. Organs* **2007**, *10*, 149-157.

19. Kim, J.; Park, Y.; Yoon, T.H.; Yoon, C.S.; Choi, K. Phototoxicity of CdSe/ZnSe quantum dots with surface coatings of 3-mercaptopropionic acid or tri-n-octylphosphine oxide/gum arabic in Daphnia magna under environmentally relevant UV-B light. *Aquat. Toxicol.* **2010**, *97*, 116-124.

20. Lu, Z.; Li, C. M.; Bao, H.; Qiao, Y.; Toh, Y.; Yang, X. Mechanism of antimicrobial activity of CdTe quantum dots. *Langmuir* **2008**, *24*, 5445-5452.

21. Su, Y.; He, Y.; Lu, H.; Sai, L.; Li, Q.; Li, W.; Wang, L.; Shen, P.; Huang, Q.; Fan, C. The cytotoxicity of cadmium based, aqueous phase-synthesized, quantum dots and its modulation by surface coating. *Biomaterials* **2009**, *30*, 19-25.

22. Su, Y.; Hu, M.; Fan, C.; He, Y.; Li, Q.; Li, W.; Wang, L.; Shen, P.; Huang, Q. The cytotoxicity of CdTe quantum dots and the relative contributions from released cadmium ions and nanoparticle properties. *Biomaterials* **2010**, *31*, 4829-4834.

23. Hezinger, A.; Teßmar, J.; Göpferich, A. Polymer coating of quantum dots—A powerful tool toward diagnostics and sensorics. *Eur. J. Pharm. Biopharm.* **2008**, *68*, 138-152.

24. Williams, D.; Ehrman, S.; Pulliam Holoman, T. Evaluation of the microbial growth response to the inorganic nanoparticles. *J. Nanobiotechnol.* **2006**, doi: 10.1186/1477-3155-4-3.

25. Jiang, G.; Shen, Z.; Niu, J.; Bao, Y.; Chen, J.; He, T. Toxicological assessment of TiO_2 nanoparticles by recombinant Escherichia coli bacteria. *J. Environ. Monit.* **2011**, *13*, 42-48.

26. Neogi, A.; Ghosh, S.; Li, J.; Cai, T.; Hu, Z. Enhanced luminescence efficiency from hydrogel microbead encapsulated quantum dots. *Mater. Res. Soc. Symp. Proc.* **2007**, *959*, 202-207.

27. Häfeli, U.; Riffle, J.; Harris-Shekhawat, L.; Carmichael-Baranauskas, A.; Mark, F.; Dailey, J.; Bardenstein, D. Cell uptake and *in vitro* toxicity of magnetic nanoparticles suitable for drug delivery. *Mol. Pharm.* **2009**, *6*, 1417-1428.

28. Frimpong, R.; Hilt, J. Poly(n-isopropylacrylamide)-based hydrogel coatings on magnetite nanoparticles via atom transfer radical polymerization. *Nanotechnology* **2008**, *19*, 175101.

29. Helbig, K.; Grosse, C.; Nies, D. Cadmium toxicity in glutathione nutants of *Escherichia coli. J. Bacteriol.* **2008**, *190*, 5439-5454.

30. Lovrić, J.; Bazzi, H.; Cuie, Y.; Fortin, G.; Winnik, F.; Maysinger, D. Differences in subcellular distribution and toxicity of green and red emitting CdTe quantum dots. *J. Mol. Med.* **2005**, *83*, 377-385.